FACULTY OF CIVIL ENGINEERING CTU IN PRAGUE

Czech Technical University in Prague
Faculty of Civil Engineering
Department of Mechanics
Thákurova 7, 166 29, Praha 6

MALCOLM 2.0
Multi-spiral Column Simulation Module

Program documentation

TAČR-MOST Project CeSTaR 2:
Reducing material demands and enhancing structural capacity of multi-spiral reinforced concrete columns - advanced simulation and experimental validation

Author: P. Havlásek
ORCID: 0000-0002-7128-3664
petr.havlasek@cvut.cz

December 2022

Report No. TM01000059-V2

Contents

1 Scope

The interaction diagram of a cross section presents an envelope of all statically admissible combinations of internal forces. In the case of columns, this is usually axial compression (normal force), N, and one or two bending moments, M_y and M_z. Such a diagram is very convenient to verify that the cross section can sustain the design load. Typically, this is done graphically; the condition is satisfied if the point corresponding to the given combination $[N,\ M_y,\ M_z]$ lies inside the interaction diagram. Especially in the precast concrete industry, highly optimized structural elements are produced in large series. Therefore, the cross section of such an element is likely to become subject to numerous combinations corresponding to various loading states. Therefore, an efficient means of verification is a must.

For conventionally reinforced concrete columns, the interaction diagram can be constructed easily by following a guideline in a particular design code [2, 7, 1]. However, for novel multi-spiral reinforcement (MSR) [20], see Fig. 1, there is no such recommendation. This prohibits making use of the superb structural performance originating from passively confined concrete and which exceeds the resistance of standard columns by approx. 25%.

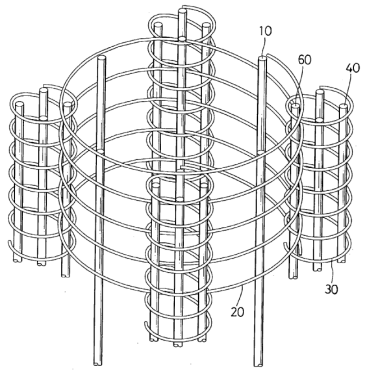

Figure 1: Multi-spiral reinforcement layout in the original U.S. patent of Samuel Yin [20].

The aim of program MALCOLM is to assist structural engineers by providing them with a newly developed guideline, tailored specifically for MSR columns. Everything is wrapped up in an accessible and friendly graphical user interface. Using this approach, key input parameters–the topology of the reinforcement and the material properties of concrete and steel–can be tuned to deliver the interaction diagram that satisfies all design load combinations. This should result into immediate material savings as their potential is utilized more efficiently. The resulting interaction diagram can be subsequently compared with the diagram constructed from nonlinear simulations, which is done here in the open source OOFEM finite element package [17, 18]. For more information, please refer to the recommendation [11].

2 Program usage

The program MALCOLM is written completely in Python 3, the GUI uses the Python module PySide2 which provides access to the complete Qt 5.12+ framework. The program is maintained on Github and is released under the LGPL 2.1 license. The program usage is free of charge for research, educational, or study purposes. The license for commercial use can be obtained upon request from the program developer.

In Linux terminal, the program is started by typing

```
$ python3 malcolm.py
```

The graphical user interface is composed of three main parts organized in columns (see Fig. 2):

1. Topology Specification
2. Interaction Diagram + Materials
3. FEM Definition

In this order, the user is guided through the design process and subsequent FEM verification. Within every part, the expected workflow and the order of definitions are from the top downward. The tags of the majority of the buttons are self-explanatory; however, the following three Sections explain the key program features in more detail.

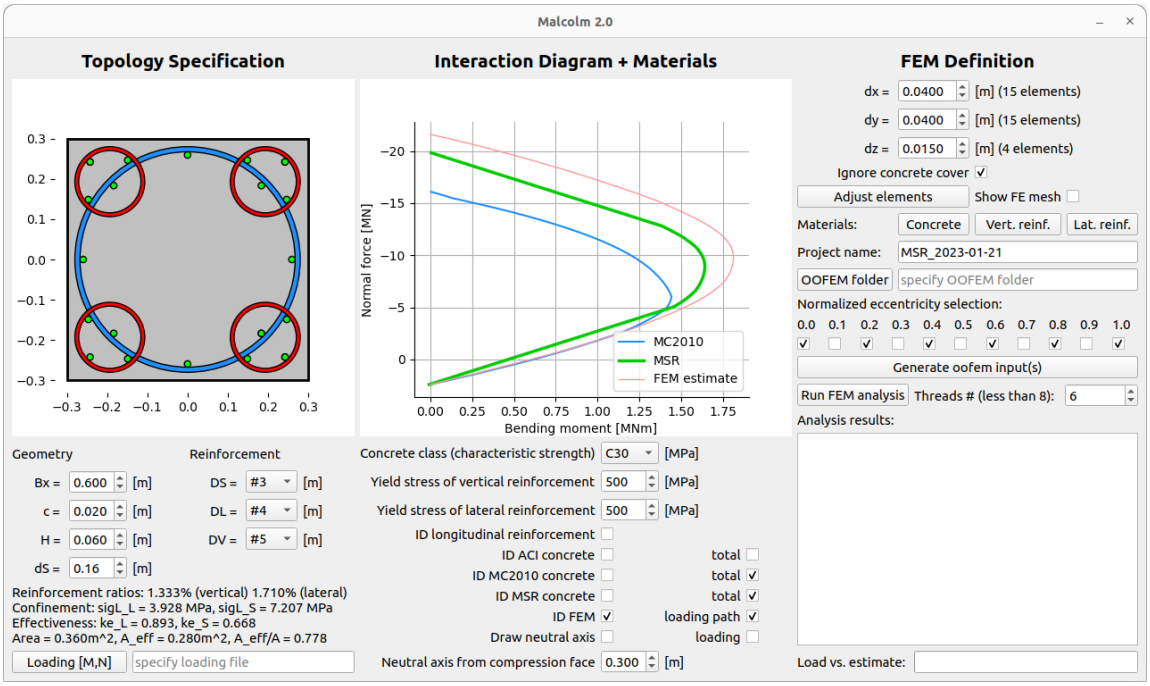

Figure 2: MALCOLM graphical user interface.

2.1 Topology Specification

The parameters listed in Table 1 are needed to uniquely specify the geometry of the cross section and reinforcement, as shown in Fig. 3. The diameter d_L follows from the width of the cross section of the column B, the concrete cover c, and the diameter of the rebar D_L because it is assumed that the objective is to design the columns with the best structural performance achieved at a maximum value of d_L. Note that the diameters d_S and d_L refer to the axial and NOT the outer diameter of the spirals.

Table 1: Notation of a square cross section with multi-spiral reinforcement. Note that d_L is not a primary parameter as it follows from column width B and concrete cover c.

Symbol	Meaning
B	column width (square cross section)
H	spiral pitch
c	concrete cover
d_L	axial diameter of the large spiral
d_S	axial diameter of small spirals
D_L	rebar diameter of the large spiral
D_S	rebar diameter of small spirals
D_V	vertical rebar diameter

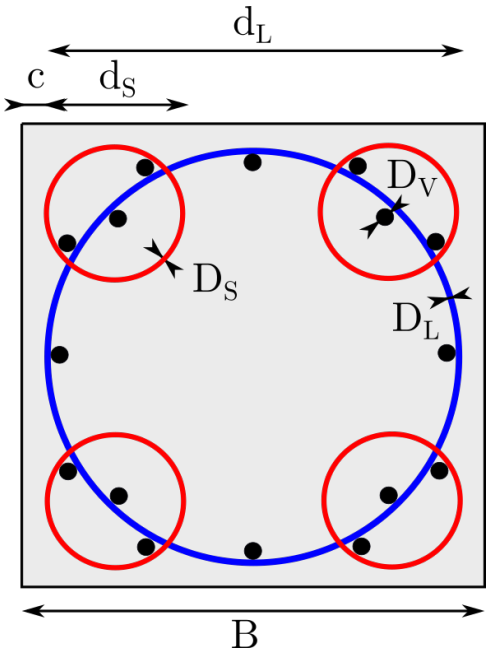

Figure 3: Schematic representation of a square cross section reinforced with multi-spiral reinforcement and definition of a notation.

The change in geometry and reinforcement invokes automatic redrawing of the column cross section and updating of the main quantities which are listed below the topology definition:

- volumetric reinforcement ratio in vertical (longitudinal) and horizontal (transverse) directions,
- average confinement produced by large spiral (`sigL_L`) and small spiral (`sigL_S`),
- confinement effectiveness factors `ke_L` and `ke_S` for large and small spirals, respectively, and
- total area of the cross section, confined area (delimited by the centerlines of the spirals), and their ratio.

Finally, the user-defined combinations of bending moment and normal force can be uploaded (either through the selection dialog `Loading [M,N]` or manually `specify loading file`. Tab-separated *.csv file containing two columns with "N" and "M" (in arbitrary order) tags in the first line. Note that the sign of normal force should follow standard convention; a positive sign stands for tension, and a negative sign for compression.

Change in the topology and reinforcement, as well as the combinations of internal forces, are automatically projected in the interaction diagram in the second (middle) part.

2.2 Interaction Diagram + Materials

The interaction diagrams (ID) are immediately being redrawn upon change in topology, reinforcement, and material properties which are:

1. **Concrete class** which corresponds to the value of the characteristic strength in compression on cylinders 150×300 mm at the age of 28 days. Conventional concrete classes from C20 (i.e., mean strength $f_{cm} = 28$ MPa) to C50 (i.e., $f_{cm} = 28$ MPa) are supported. The default value is C30 ($f_{cm} = 38$ MPa).
2. Yield stress of **vertical reinforcement** in MPa, default value is 500 MPa.
3. Yield stress of **lateral reinforcement** in MPa, default value is 500 MPa.

The interaction diagram corresponds to the mean (i.e., neither characteristic nor design resistance). The following ways for evaluating the interaction diagrams can be selected:

1. ID for longitudinal (i.e., vertical) reinforcement.
2. ID according to ACI-318 (either total resistance or concrete only), no influence of confinement or transverse reinforcement is considered.
3. ID according to *fib* MC2010 (either total resistance or concrete only), no influence of confinement or transverse reinforcement is considered.

4. ID with formulae according to/inspired by *fib* MC 2010 (for details, see Section 3.2 or [11]) which considers the effect of lateral confinement on concrete strength. The total resistance or the contribution only due to concrete can be selected. The diagram is shown in two colors:

   - The diagram, which does not consider any contribution of concrete cover and thus should be used **for design**, is shown in **green**.
   - The larger diagram shown in thin **pink** lines partially considers concrete cover: the corners of the cross section are not rounded but sharp and the transition between large and small spirals is straight and not rounded. This diagram is intended for **comparison with FEM model** which uses the same topology.

5. The checkboxes `ID FEM` and `loading path` are checked by default but become effective once the first FEM analysis is completed. The first control switches on and off the interaction diagram obtained via FEM simulations in the OOFEM program. The latter shows the results for the individual loading steps whose individual distance decreases as the FEM estimate is approached. The computed vertices of the interaction diagram can be identified by the value of normalized eccentricity $\hat{e} = e/(B/2)$ and the corresponding coordinates [M,N].

Additionally, the response for a particular position of the neutral axis can be shown in the selected diagrams. The position is controlled by modifying the distance from the compressed fibers (top side of the cross section in Topology Specification part).

The checkbox `loading` toggles on and off the visibility of user-specified [M,N] loading combinations.

2.3 FEM Definition

The last part allows us to specify the computational model to be generated and subsequently computed in FE package OOFEM. The finite element sizes of the structure element model in the direction x, y (horizontal), and z (vertical) are specified in the boxes `dx`, `dy`, `dz`. Upon clicking `Adjust elements`, the actual element size is automatically modified to satisfy a uniform distribution. The numbers in parentheses next to the edit boxes specify the number of elements in respective directions. After generation (clicking `Adjust elements`), the mesh in the plan view is shown if the box `Show FE mesh` is checked. Please note that in the case of MSR, the results are mesh-sensitive, and the comptued load decreases with mesh refinement.

The default behavior of the constitutive models for concrete, vertical, and lateral reinforcement can be adjusted next. In the case of concrete, the behavior is described by CDPM2 [9] whose parameters are automatically generated from the mean value of compressive strength, f_{cm} which is inferred from the concrete class. A summary of this constitutive model is presented in Section 3.3.2.

Similarly, the reinforcement yield stress follows from its earlier definition. With default settings, the material behavior of steel is ideally elastoplastic without hardening; the meaning of the material parameters is described in Section 3.3.3.

Text field `Project name` which defines the name of the parent folder for computations will be specified next. The default name contains the current date. If the project name already exists, the contents of the folder will be deleted.

The button `OOFEM folder` opens a dialog for selecting OOFEM project compiled with the parameter `USE_PYBIND_BINDINGS` set `ON`. (The folder must contain `oofempy.so`.) The other requirement is the direct spare solver (`USE_DSS`) which delivers together with the elastic stiffness matrix the most robust and computationally very efficient solution.

Checkboxes with values of normalized eccentricity $\hat{e}$ determine the simulations that will be executed to construct the interaction diagram via FEM. Experience indicates that a set of 6 simulations ranges from 0.0 to 1.0 with 0.2 steps is sufficient (default settings). Once the geometry, material properties, and eccentricities have been specified, the OOFEM input files can be generated. The individual problems will be created in the parent project folder, and the name coincides with the value of eccentricity.

Provided the OOFEM configuration has been done with `USE_OPENMP` set `ON`, the analysis can be run in parallel. The default number of threads is set to 3/4 of the maximum.

`Run FEM analysis` triggers the sequence of finite element simulations which start from the lowest value of selected eccentricity. Progress bar `Load vs. estimate` shows the ratio of the current load level related to the estimate for given eccentricity. `Analysis results` window shows the progress of the currently running simulation. The load level is the value of normal force in MN. All simulations are terminated once the load level starts decreasing. Upon finishing, the window summarizes the results (eccentricity, normal force, bending moment). Two snapshots are shown in Fig. 4.

The time needed for one simulation differs according to the user-defined settings (especially materials definition, density of the finite element mesh, and the number of available cores for parallel execution). In general, the computational time increases with eccentricity. During testing, one simulation in uniaxial compression took approximately 2-5 minutes.

Once the individual analysis has been completed, the `*.vtu` results can be processed graphically, e.g., in Paraview.

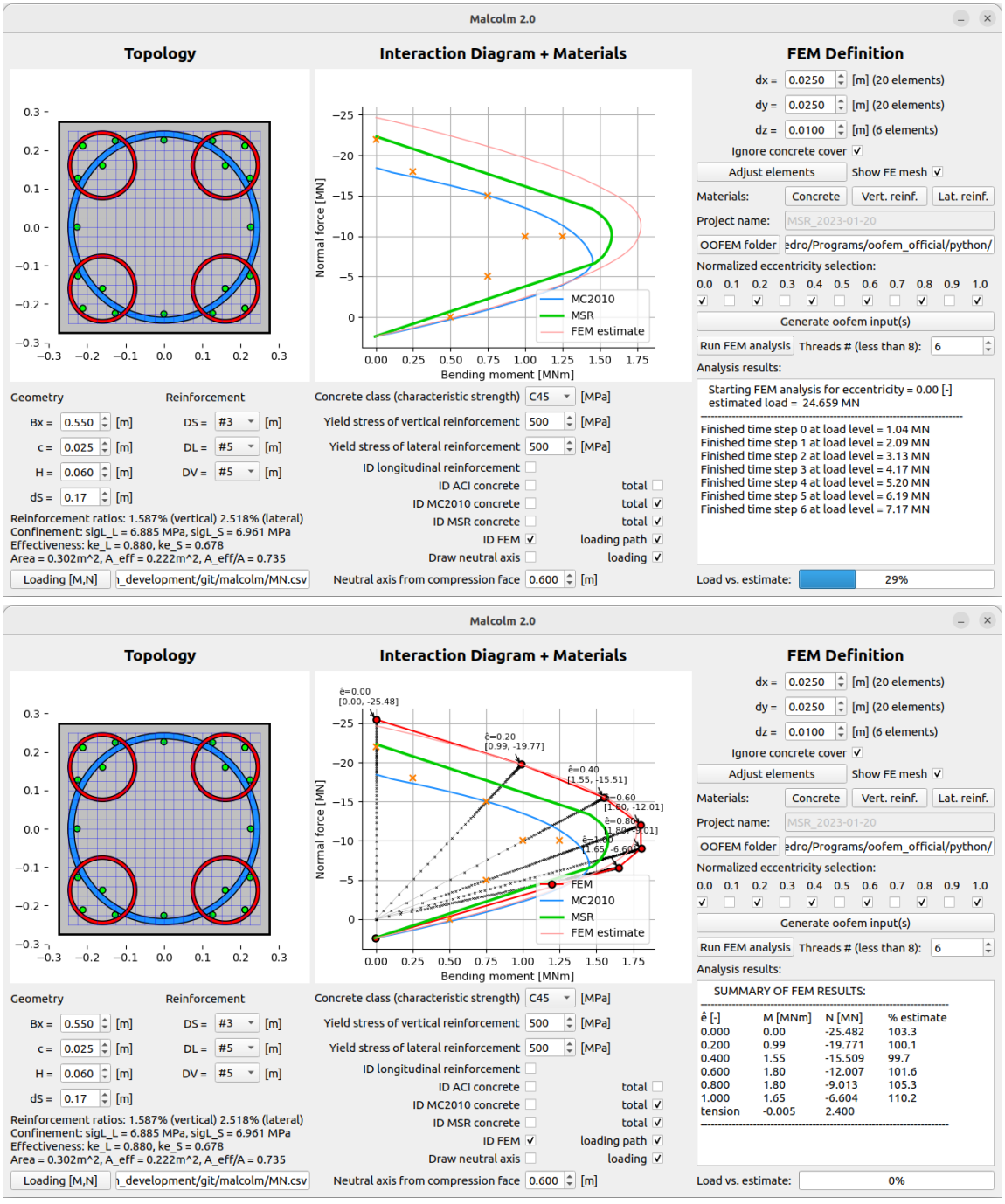

Figure 4: Snapshots of the GUI MALCOLM during the running analysis (top) and once all selected problems have been completed (bottom).

3 Background

3.1 Behavior of concrete under passive confinement

In most structural applications, transverse reinforcement invokes confinement in response to lateral expansion of the concrete. Lateral expansion is both elastic (Poisson effect) and inelastic (plastic deformation and microcracking). The confinement builds up from zero in the unloaded state to its ultimate value given by the reinforcement layout, volume, and material characteristics. As this kind of confinement depends on another action, it is called *passive* confinement.

The equations for the strength of elements with passively confined concrete, embedded in the design codes and recommendation, usually comprise two fundamental components: i) the influence of the reinforcement layout, dimensions, and material properties on the magnitude and distribution of lateral confinement, and ii) the effect of lateral confinement on concrete strength. Typically, a single parameter called the "confinement effectiveness factor", k_e, is used to capture the efficiency of the stress transfer from transverse reinforcement to concrete.

In a circular column reinforced with hoops, the average value of passive lateral confinement σ_L (compression treated as positive) can be more easily derived from the equilibrium condition of the stress resultants of confined concrete and the yielding reinforcement (in tension).

$$\sigma_L = \frac{2A_{\varnothing} f_y}{DH} \tag{1}$$

In the above equation, $A_{\varnothing}$ is the cross-sectional area of the reinforcement bar, f_y is its yield strength, D is the diameter (center-line) and H is the vertical spacing of the hoops. This expression is also applicable for spiral reinforcement, in this case H denotes the spiral pitch. (One might reflect the fact that the axial force in the spiral reinforcement is not oriented horizontally, but in practical applications the difference is rather insignificant.)

3.1.1 Confinement efficiency

The distribution of lateral confinement is strongly influenced by the layout of the transverse reinforcement, in particular by the ratio H/D. The design codes and recommendations derived from Mander's model [15] presume that the concrete bound by the center line of the spiral or circular loop can be divided into unconfined and effectively confined regions, while the concrete cover, which tends to spall off at very small axial strains, can be neglected as it does not contribute to the ultimate carrying capacity. In the case of axial compression, the distribution of vertical (axial) stress in the confined and unconfined parts (individually) is idealized as uniform.

Based on this hypothesis, the influence of lateral reinforcement on the distribution of lateral confinement can be conveniently incorporated into engineering computations through a simple multiplicative factor called confinement effectiveness.

$$k_e = \sigma'_L / \sigma_L \tag{2}$$

where σ'_L is the effective lateral compressive stress (confinement). Initially, k_e was motivated by the ratio

$$k_e = A'_c/A_c \tag{3}$$

(which is used in the draft of the new EC2) where A'_c and A_c are the areas of confined and total concrete in the weakest section of the column, respectively. The latter approach which returns to the initial definition is preferred here, but—as shown in [11]—the differences between the two approaches are not significant.

Extensive numerical study [10] has revealed that the effectiveness factor is very similar for the reinforcement with spiral and circular hoops. The factor perfectly matches a simple rule

$$k_e = \left(1 - \frac{H}{2D}\right)^2 \tag{4}$$

This expression was originally derived for reinforcement with hoops under the assumption of parabolic distribution of lateral confinement.

3.1.2 Concrete strength under confinement

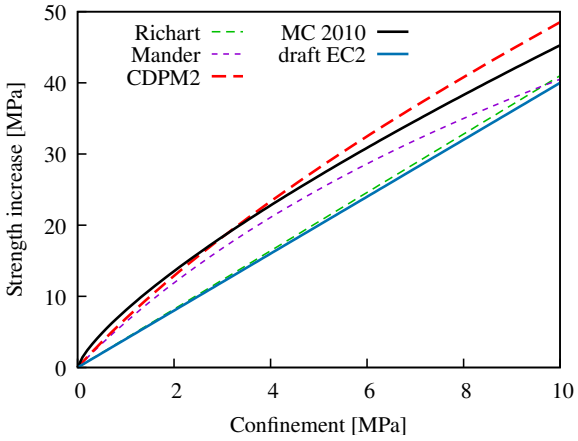

Figure 5: Comparison of design codes for concrete with compressive strength 28 MPa: increase in strength due to ideally distributed lateral confinement.

The increase in concrete strength due to (imperfect) confinement according to *fib* Model Code 2010 is given by

$$\Delta f_{c,c} = 3.5\,(k_e \sigma_L)^{3/4}\, f_c^{1/4} \tag{5}$$

In a typical range of applications, $\sigma_L < 10$ MPa, the results of models describing the increase in strength due to confinement, presented above, are very similar to Richart's recommendation from 1929 [5], $\Delta f_{c,c} = 4.1\sigma_L$, as shown in Figure 5.

This Figure also shows the response obtained with CDPM2, which is used in FEM analyzes (Section 3.3.2) and gives the highest increase in strength. Provided that the

value of the tensile strength f_t is estimated according to MC 2010 (14), the increase in strength due to the confinement of CDPM2 can be accurately approximated by

$$\Delta f_{c,c} = 7.65\sigma_L^{0.80}\left[1 + 0.0085\left(f_c/\text{MPa} - 28\right)\right] \tag{6}$$

in which a power function is multiplied by a strength correction term that is set to 1.0 when $f_c = 28$ MPa [10].

3.1.3 Stress-strain diagram for confined concrete

The Model Code 2010 provides an enhancement of the compressive strength[1] and an increase in the characteristic strain under confinement only for the parabola-rectangle stress-strain diagram. The compressive strength $f_{c,c}$ under effective confinement σ_L is reached at strain

$$\varepsilon_{c2,c} = \varepsilon_{c2}\left[1 + 5\left(\frac{f_{c,c}}{f_c} - 1\right)\right] \tag{7}$$

The expression for the ultimate strain under confinement reads

$$\varepsilon_{cu2,c} = \varepsilon_{cu2} + 0.2\sigma_L/f_c \tag{8}$$

The reference values of the strain are constant for concrete grades up to 50 MPa: $\varepsilon_{c2} = 2 \times 10^{-3}$ (compression), and $\varepsilon_{cu2} = 3.5 \times 10^{-3}$ (compression).

The complete stress-strain diagram consists of a second-order parabola (up to ε_{c2})

$$\sigma_c = f_{c,c}\left[1 - \left(1 - \varepsilon_c/\varepsilon_{c2,c}\right)^2\right] \quad \text{for} \quad 0 \le \varepsilon_c \le \varepsilon_{c2,c} \quad \text{(compression)} \tag{9}$$

which is followed by a constant plateau (up to $\varepsilon_{cu2,c}$).[2]

$$\sigma_c = f_{c,c} \quad \text{for} \quad \varepsilon_{c2} \le \varepsilon_c \le \varepsilon_{cu2} \quad \text{(compression)} \tag{10}$$

[1] Design and characteristic strength were replaced by the mean strength

[2] The same two equations define the stress-strain diagram in Eurocode 2; the only difference is the value of concrete strength under given confinement.

3.2 Interaction diagram for MSR columns: hand calculation

3.2.1 General design principles and rules for efficient design

The rules for the analysis of reinforced concrete columns in Taiwan are largely based on the American ACI-318 [2]. This building code postulates two criteria on lateral reinforcement which must be satisfied: i) the strength criterion guarantees that the structural resistance is maintained if the concrete cover spalls off, ii) the ductility criterion guarantees sufficient rotation capacity for structures in seismic areas. This set of rules was developed for columns with conventional layout of transverse reinforcement; however, in the case of MSR which provides superior structural response, these requirements lead to unnecessary overdesign.

The Taiwanese national amendment [4] sets additional criteria on the topology of multi-spiral reinforcement. The maximum distance between the inner faces of the overlapping spirals should exceed 0.3 times the inner diameter of the smaller spiral (or 60 mm). Based on the master thesis of Kuo [14], the ratio of the outer diameters of the small and large spirals should be 0.3:1.

3.2.2 Methodology

This section proposes a simplified methodology for estimating the interaction diagram of concrete columns with square cross section and multi-spiral reinforcement. The constitutive model for confined concrete adopted here is that from Model Code 2010; however, several modifications are introduced in certain aspects to produce satisfactory results which comply with the lessons learned from the numerical simulations [11].

In principle, the procedure for evaluating the interaction diagram for columns with multi-spiral reinforcement is straightforward. The calculation consists of a repetitive evaluation of the integral internal forces (normal force and bending moment/s) which are the resultants of the stress distribution obtained for various selections of the neutral axis and for a prescribed value of strain at the compressive fibers. The position of the neutral axis is varied, starting at the compression face throughout the cross section, until reaching the state when the entire cross section is in (almost) uniform compression, which is the case for the neutral axis placed outside the cross section.

3.2.3 Algorithm: Interaction diagram for the design of columns with multi-spiral reinforcement

The algorithm for constructing the interaction diagram for columns with multi-spiral reinforcement was formulated with the objective to optimally balance the complexity and accuracy. The main assets of the algorithm are

i) Given the simplified assumptions, whose justification can be found in [11] or the design codes, the algorithm gives the exact solution.

ii) The form of all formulae can be readily presented in closed-form expressions. This presents a great benefit, which simplifies the implementation in spreadsheets.

iii) The algorithm can be evaluated very efficiently, which promotes the incorporation of an optimization algorithm for an efficient design of topology and/or material properties.

iv) The exceptional accuracy of the proposed algorithm has been assessed by nonlinear finite element simulations with advanced constitutive models for concrete and steel.

The entire procedure has been implemented in the MALCOLM 2.0 program.
The algorithm is composed of the following steps; please refer to Fig. 6:

1. Define the topology of the cross section and the material properties.
2. Determine the values of the single-confined area A^S, double-confined area A^D, and the positions of their centroids. The values should be associated with the centerlines of small and large spirals.
3. From (1) compute the confinement efficiency factors k_e^S, k_e^L, and $k_e^D = \min(k_e^S, k_e^L)$.
4. Using the equilibrium condition (1), compute the average confinement σ_L^S, σ_L^L, and $\sigma_L^D = \sigma_L^S + \sigma_L^L$.
5. For every region L, S, D evaluate the increase in strength due to confinement $\Delta f_{c,c}(\sigma_L)$ following the MC 2010 formula (5) with $k_e = 1$.
6. Using the empirical formula (4), find the minimum value of effective confinement (either for the small or large spiral), and use this value in Equation (8) to calculate the ultimate strain $\varepsilon_{cu2,c}$. Assign this strain to the borderline of the confined section; see Fig. 6.
7. For every position of the neutral axis x do the following steps. (The neutral axis should be chosen so that the line λx does not intersect small spirals, using $\lambda = 0.875$ independently of the topology and reinforcement configuration [11].)
   (a) Find the single confined area A^L of the large spiral and its centroid (shown in blue in Fig. 6), which is cropped by the line λx and further reduced by the overlapping parts of small spirals.

(b) Using the concept of an effective confined area equation (3), evaluate the stress resultant on the individual areas A^S, A^L and A^D. The confining stresses in the double-confined regions are assumed to be additive and the smaller value of k_e should be taken. Note that the uniaxial compressive strength is assumed on the entire area A^i, while the increase due to confinement is only on the effective part $k_e A^i$ with the same centroid.

(c) Sum the contributions of all stress resultants to get the combination $[M, N]$ for one position of the neutral axis.

(d) Add the contribution of longitudinal reinforcement, assume linear distribution of strain over the cross section.

8. Add the results for two special cases of uniaxial compression and uniaxial tension.

9. Connect the points to construct the interaction diagram.

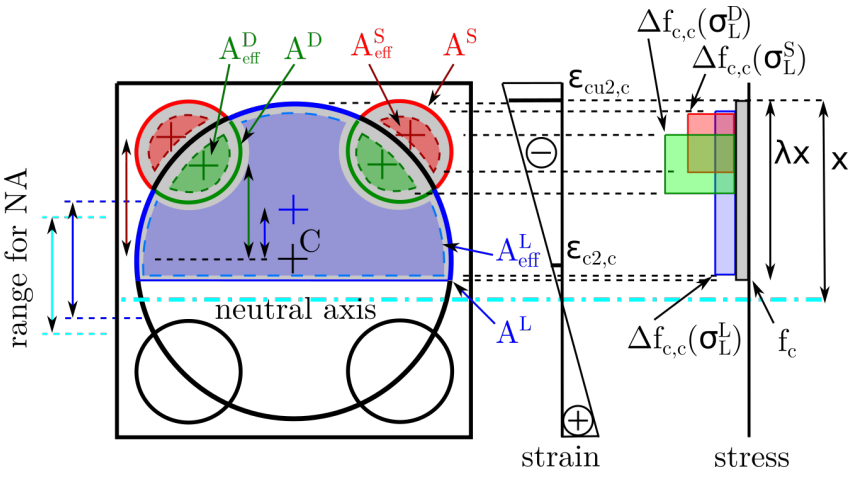

Figure 6: Square MSR cross section subject to eccentric compression: assumed distribution of strain and resulting strain associated with the ultimate limit state.

Figure 7 presents a comparison of the conventional concept that does not consider confinement (MC2010, black line) with the result obtained using the presented algorithm (MSR, thick green line). One can immediately see the increase of approx 25% which remains constant between the balance point and pure compression.

3.2.4 Validation of the interaction diagram via finite element analysis

The constructed interaction diagram can be validated at no cost via nonlinear finite element simulations. To achieve realistic spalling of the concrete cover and at the same time to preserve smooth convergence of the simulation is next to impossible.

To overcome this obstacle and to obtain a reasonable agreement, one needs to adopt a similar modeling concept, which does not consider the contribution of the concrete cover.

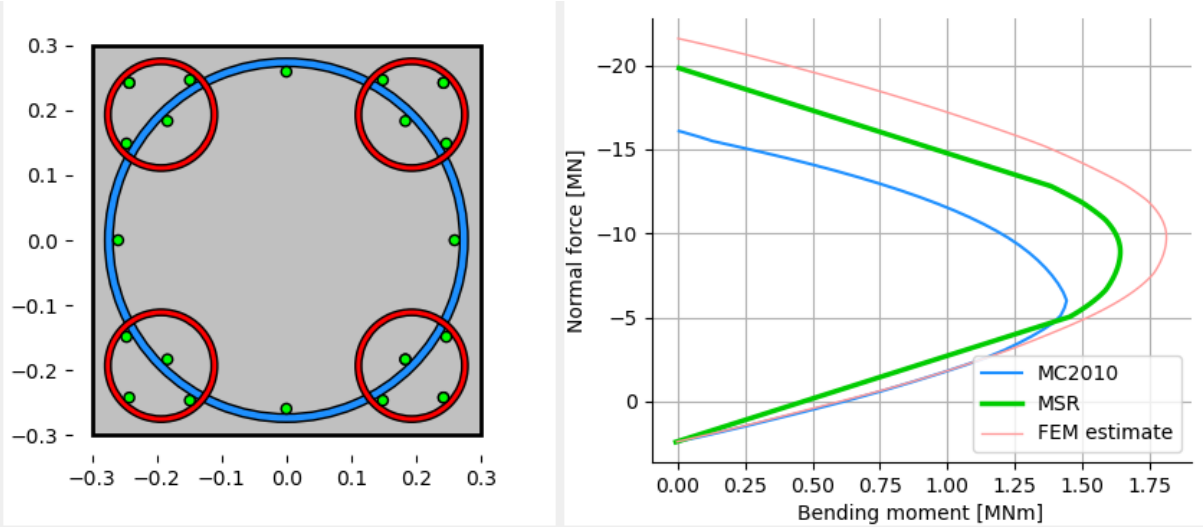

Figure 7: Interaction diagrams evaluated for square cross sections given by $B = 0.6$ m, $c = 0.02$ m, $H = 0.06$ m, $d_S = 0.16$ m, D_S =#3, D_L =#4, D_V =#5, $f_{cm} = 38$ MPa, $f_y = 500$ MPa.

However, creating a structured yet irregular mesh that conforms to the border of the confined region presents a challenge.

To offer a reasonable trade-off, the previous algorithm can be adjusted and in a sense simplified, as documented in Fig. 8. The finite element mesh can remain perfectly regular if a certain contribution of concrete cover is incorporated into the algorithm as shown in gray color. (Otherwise, the domain of the computational model is offset by the thickness of the concrete cover c.)

Omitting the double-confined region allows the neutral axis to travel throughout the entire depth of the cross section. (Of course, one admits that full confinement can develop even in partially compressed spirals.) Naturally, ignoring the nonlinearity between confinement and concrete strength would lead to a certain, yet acceptable, overestimation of the strength.

The resulting curve, which can be objectively compared with the finite element simulations with regular mesh, is shown in Fig. 7 in a thin pink line.

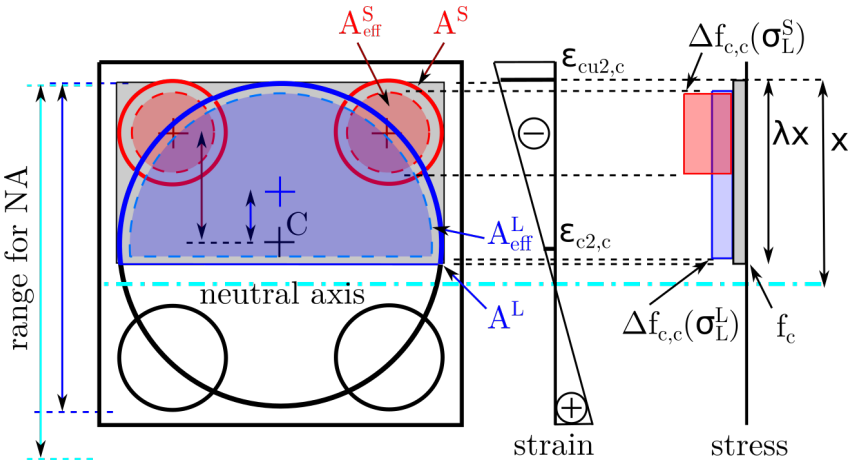

Figure 8: Square MSR cross section subject to eccentric compression: simplified approach used for comparison with FEM simulations, which partially considers stress in concrete cover.

3.3 Interaction diagram for MSR columns: FEM analysis

3.3.1 Methodology

More accurate yet computationally more demanding approach to construct the interaction diagram for columns with multi-spiral reinforcement uses a set of repeatedly run nonlinear finite element simulations in which a representative section of the column is subject to different load scenarios [12].

An example of such a representative section is illustrated in Fig. 9; as shown, the height of the model is equal to one spiral pitch. Suitable boundary conditions must be assigned to both the top and bottom surfaces to guarantee realistic behavior. The model uses a generalized master-slave condition to impose periodicity in the axial direction of the column. In the horizontal direction, the nodal displacements on the top horizontal surface are fully linked to the corresponding degrees of freedom on the bottom surface; otherwise the lateral deformation is not restrained as depicted in Fig. 9 by the rollers. In the vertical direction, the displacement on the bottom surface is fixed, while on the top surface it obeys a kinematic condition which allows the vertical displacement of the entire surface and its rotation about both horizontal axes. Provided that the failure mode is not localized, this approach [13] enables introducing a significantly denser FE mesh than when modeling the entire column, and thus identifying subtle differences thoroughly among various reinforcement alternatives. The mesh of the finite element

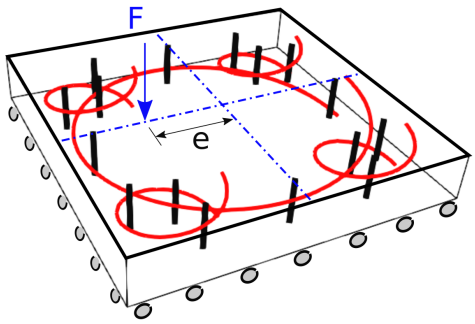

Figure 9: Computational model of a representative section.

model combines a structured mesh (e.g., linear hexahedral elements) with regularly and irregularly discretized longitudinal and spiral reinforcement (linear truss elements). The two meshes are interconnected using the concept of hanging nodes, and the bond between concrete and steel is treated as rigid. The disabled slip is justified by the assumption that the tensile force in the steel spirals should be almost uniform over the length, at least when the entire spiral is in compression.

There are two different approaches to subject the first computational model to the combination of normal force and bending moment. The loading can be defined by means of an eccentric force; in such a case, the ratio between the bending moment and normal

force remains constant; therefore, in the M-N graph, the loading path is a straight line that reaches the interaction diagram at the maximum value of the loading force. In the other approach, the loading can be defined by a fixed ratio of axial deformation and curvature. Then the response becomes highly nonlinear as the loading path approaches the interaction diagram, which might not be reached at the maximum load. This implies that in the latter approach, the interaction diagram needs to be extracted as a convex shape of all computed responses, which is not favorable. For this reason, loading with a single force F with prescribed eccentricity e should be preferred.

Exceptional agreement of the modeling concept and the Algorithm listed in the previous Section is shown in Fig. 4. Solid green line is the estimated interaction diagram if the contribution of concrete cover is completely neglected. If the corners and the regions between the small and large spirals are added, the strength increases, as illustrated by the solid pink line. Yet this strength envelope is in perfect agreement with the FEM analysis (thick red line and circular marks) whose regular finite element mesh is shown in the left part of the figure.

3.3.2 Damage-Plastic Model for Concrete Failure, CDPM2

Concrete behavior is captured by the CDPM2 [9] (Con2DPM in OOFEM). The model capabilities cover all crucial aspects which are necessary for realistic modeling columns with multi-spiral reinforcement: i) correct evolution of volumetric strain, which is essential for the development of passive confinement, ii) confinement-dependent hardening, and iii) post-peak softening. The performance of this model was recently extensively validated [10] against experimental data from the literature on both actively and passively confined concrete.

The model is based on plasticity with isotropic hardening and non-associated flow [8], combined with a scalar damage model with damage driven by plastic flow and elastic strain. The yield condition inspired by Warnke [19] and [16] is formulated in the effective stress space and depends on all three stress invariants. The flow rule is derived from a plastic potential that depends on the hydrostatic stress and the second deviatoric invariant.

The model deals with the effective stress

$$\bar{\boldsymbol{\sigma}} = \boldsymbol{D}_e(\boldsymbol{\varepsilon} - \boldsymbol{\varepsilon}_p) \tag{11}$$

which is computed using the plastic part of the model. Here, $\boldsymbol{D}_e$ is the elastic material stiffness matrix, $\boldsymbol{\varepsilon}$ is the total strain and $\boldsymbol{\varepsilon}_p$ is the plastic strain.

The model uses two independent scalar damage variables ω_t and ω_c for tension and compression, respectively, which allow for the transition from effective to nominal stress. To achieve that, the effective stress is first split into the positive part, $\langle\bar{\boldsymbol{\sigma}}\rangle_+$, and the negative part, $\langle\bar{\boldsymbol{\sigma}}\rangle_-$. Subsequently, the nominal stress is computed as

$$\boldsymbol{\sigma} = (1-\omega_t)\langle\bar{\boldsymbol{\sigma}}\rangle_+ + (1-\omega_c)\langle\bar{\boldsymbol{\sigma}}\rangle_- \tag{12}$$

The softening curve in tension is derived from a bilinear traction separation law characterized by the tensile strength, the fracture energy, and the position of the midpoint defined by two dimensionless ratios w_{f1}/w_f and σ_1/f_t.

To prevent mesh-dependent results, the model in the present study is regularized by a crack-band approach [3] (adjustment of a parameter that controls damage propagation depending on the size of the finite element).

The constitutive model uses a large number of parameters. The parameters which have a clear physical meaning can be estimated using, e.g., the *fib* Model Code 2010 [6] from the mean value of compressive strength f_{cm}. Following these recommendations, the approximate value of the initial modulus (in GPa) can be computed using

$$E_{ci} = 21.5\,(0.1 f_c)^{1/3} \tag{13}$$

The bilinear traction-separation law is characterized by the tensile strength, fracture energy, and the position of the midpoint defined by two dimensionless ratios w_{f1}/w_f and σ_1/f_t (see Table 2).

Nowadays, most structural concrete meets the condition $20\,\text{MPa} \leq f_c \leq 58\,\text{MPa}$ for which the mean value of the tensile strength (in MPa) and the fracture energy (in N/m) can be calculated as

$$f_t = 0.3\,(f_c - 8\,\text{MPa})^{2/3} \tag{14}$$

$$G_F = 73 f_c^{0.18} \tag{15}$$

The remaining material parameters can be kept to their default values and are summarized in Table 2. For more information, please refer to the original paper [9] or to the updated documentation (matlibmanual) available at OOFEM github repository.

Table 2: Summary of the parameters of CDPM2 which are treated as constant in present study. All parameters are dimensionless.

Parameter	Value	Meaning
ν	0.2	Poisson's ratio
e	0.525	eccentricity
q_{h0}	0.3	initial value of hardening variable q_{h1}
H_p	0.01	hardening modulus
D_f	0.85	dilation factor
A_h	0.08	hardening parameter
B_h	0.003	hardening parameter
C_h	2	hardening parameter
D_h	10^{-6}	hardening parameter
A_s	15	softening parameter
ε_{fc}	10^{-4}	softening parameter for compression
w_{f1}/w_f	0.15	parameter for bi-linear softening in tension
σ_1/f_t	0.3	parameter for bi-linear softening in tension

3.3.3 Plasticity model for reinforcement

Currently, the most suitable material model for steel reinforcement in OOFEM is the Mises plasticity model with isotropic damage, denoted as "`MisesMat`". The model uses the Mises yield condition (in terms of the second deviatoric invariant, J_2), the associated flow rule, linear isotropic hardening driven by the cumulative plastic strain, and isotropic damage, also driven by the cumulative plastic strain.

Under default program settings, the model behavior is ideally elasto-plastic without hardening and damage.

The total strain is split into elastic and plastic parts

$$\varepsilon = \varepsilon_{\mathrm{e}} + \varepsilon_{\mathrm{p}}, \tag{16}$$

and the stress-strain law reads

$$\sigma = (1-\omega)\bar{\sigma} = (1-\omega)\mathbf{D}(\varepsilon - \varepsilon_{\mathrm{p}}), \tag{17}$$

in which $\bar{\sigma}$ is the effective stress, σ is the nominal stress, ω is the damage variable, and D is the elastic stiffness matrix.

The yield function is defined in terms of the effective stress

$$f(\bar{\sigma}, \kappa) = \sqrt{3J_2(\bar{\sigma})} - \sigma_Y(\kappa), \tag{18}$$

and the evolution of yield stress is captured by the linear hardening law

$$\sigma_Y(\kappa) = \sigma_0 + H\kappa, \tag{19}$$

in which the cumulative plastic strain is computed incrementally from the plastic strain increment.

$$\dot{\kappa} = \|\dot{\varepsilon_p}\|, \tag{20}$$

Finally, the evolution laws for the plastic strain and damage read

$$\dot{\varepsilon_p} = \dot{\lambda}\frac{\partial f}{\partial \bar{\sigma}}, \tag{21}$$

$$\omega(\kappa) = \omega_c(1 - \mathrm{e}^{-a\kappa}), \tag{22}$$

This model can be calibrated to provide both a simplified code-like bilinear stress-strain relationship as well as a realistic experimental response.

Acknowledgment

Financial support for this work was provided by the Technology Agency of the Czech Republic (TAČR), project number TM01000059 (Reducing material demands and enhancing structural capacity of multi-spiral reinforced concrete columns - advanced simulation and experimental validation).

References

[1] *Eurocode 2: Design of concrete structures – Part 1-1: General rules, rules for buildings, bridges and civil engineering structures, Final Version of PT1-draft prEN 1992-1-1 2018 D3*. 2018.

[2] American Concrete Institute. *ACI 318-19 Building Code Requirements for Structural Concrete and Commentary*. American Concrete Institute, 2019.

[3] Z. P. Bažant and B. H. Oh. Crack band theory for fracture of concrete. *Matériaux et Construction*, 16(3):155–177, May 1983.

[4] CPAMI. *Design Specifications for Reinforced Concrete Structures*. Construction and Planning Agency, Ministry of the Interior, Taiwan, 2019.

[5] F. Erwin Richart, A. Brandtzæg, and R. Lenoi Brown. Failure of plain and spirally reinforced concrete in compression. 01 1929.

[6] Fédération Internationale du Béton. *Model Code 2010*. Number vol. 65 in fib Bulletin. International Federation for Structural Concrete (fib), 2012.

[7] Fédération Internationale du Béton. *Model Code 2010 - Final draft, Volume 2*. Number vol. 66 in fib Bulletin. International Federation for Structural Concrete (fib), 2012.

[8] P. Grassl. Modelling of dilation of concrete and its effect in triaxial compression. *Finite Elements in Analysis and Design - FINITE ELEM ANAL DESIGN*, 40:1021–1033, 06 2004.

[9] P. Grassl, D. Xenos, U. Nyström, R. Rempling, and K. Gylltoft. CDPM2: A damage-plasticity approach to modelling the failure of concrete. *International Journal of Solids and Structures*, 50(24):3805 – 3816, 2013.

[10] P. Havlásek. Numerical modeling of axially compressed circular concrete columns. *Engineering Structures*, 227:111445, 2021.

[11] P. Havlásek. Recommendation for calculating the interaction diagrams for columns with multi-spiral reinforcement. Report No. TM01000059-O-2022V001, 2022.

[12] P. Havlásek, Z. Bittnar, B. Li, J. Lau, and Y. Ou. Interaction diagram for columns with multispiral reinforcement: Experimental data vs. blind prediction using cdpm2. In *Computational Modelling of Concrete and Concrete Structures*, 1, London, GB, 2022. CRC Press.

[13] P. Havlásek, M. Jirásek, and Z. Bittnar. Modeling of precast columns with innovative multi-spiral reinforcement. fib Proceedings, pages 2301–2307. FIB - Féd. Int. du Béton, 2019.

[14] M. Kuo. *Axial Compression Tests and Optimization Study of 5-Spiral Rectangular RC Columns, Master Thesis (in Chinese)*. National Chiao Tung University, Hsinchu, Taiwan, 2008.

[15] J. B. Mander, M. J. N. Priestley, and R. Park. Theoretical stress-strain model for confined concrete. *Journal of Structural Engineering*, 114(8):1804–1826, 1988.

[16] P. Menetrey and K. Willam. Triaxial failure criterion for concrete and its generalization. *ACI Structural Journal*, 92(3):311–318, 1995.

[17] B. Patzák. OOFEM home page. http://www.oofem.org, 2000.

[18] B. Patzák. OOFEM - an object-oriented simulation tool for advanced modeling of materials and structures. *Acta Polytechnica*, 52(6):59–66, 2012.

[19] K. Willam and E. Warnke. Constitutive models for the triaxial behavior of concrete. *Proceedings of the International Assoc. for Bridge and Structural Engineering*, 19:1–30, 1974.

[20] S. Yin. Helical rebar structure, 2005. US Patent 6,860,077.